PERGAMON

Journal of Structural Geology 21 (1999) 777–793

JOURNAL OF STRUCTURAL GEOLOGY

Fluid- and reaction-assisted low-angle normal faulting: evidence from rift-related brittle fault rocks in the Alps (Err Nappe, eastern Switzerland)

Gianreto Manatschal

Geologisches Institut, ETH Zentrum, CH-8092 Zürich, Switzerland

Received 5 May 1998; accepted 11 March 1999

Abstract

Brittle fault rocks associated with a rift-related low-angle detachment system, exposed in the Lower Austroalpine Err Nappe (eastern Switzerland), exhibit systematic changes in mineralogy, fabrics, and structures, which are reflected by the transition from an undeformed granite to a cataclasite and a phyllosilicate-rich gouge across the fault zone. Cross-cutting relationships between the brittle fault rocks and syn-kinematic quartz veins suggest that a major part of the 11 km (min.) of displacement along the fault zone was accommodated in the thin, continuous gouge layer.

Strain localization in the fault zone is controlled by fluid-assisted deformation which enhances break-down reactions of feldspar to phyllosilicates. An increasing proportion of phyllosilicates decreases the strength and the permeability of the fault zone and may facilitate inter-crystalline deformation mechanisms such as grain-boundary sliding in phyllosilicate-rich zones. Normal slip of the hanging wall relative to the footwall at low angles of inclination may be facilitated by weakening of the fault zone and transient high pore pressure events.

1. Introduction

An increasing number of observations record the existence of low-angle detachment faults which were active in the brittle upper crust (e.g. Wernicke, 1995; Albers et al., 1997). However, their significance remained highly controversial because they are apparently in conflict with the basic rules of mechanics. Anderson's theory (Anderson, 1951) predicts extensional faults to be active at high angles of about 60° in the brittle upper crust. A key to explain the controversy between observations and current theory might be the study of fault rocks, because these are intimately related to the process of faulting.

Fault rocks from large-scale fault zones result from the interaction between deformation processes and syn-kinematic prograde or retrograde metamorphic reactions, all dependent on temperature, pressure, strain, strain rate, and availability of fluid. Since the boundary conditions controlling the evolution of fault rocks show temporal and spatial variations along a fault zone, neither the results of experimental studies which are commonly difficult to translate to the scale of a real fault zone, nor studies of naturally formed fault rocks alone, which commonly record a complex and ambiguous strain history, allow an understanding of the processes occurring along fault zones. Furthermore, the complex relationship between deformation, the action of fluids and retrograde alteration processes, the latter being specifically relevant for extensional systems, is not yet well understood. Because retrograde mineral reactions are usually kinetically hindered in experiments, the interplay between deformation and retrograde alteration is difficult to simulate in the laboratory and its evaluation depends consequently also on studies of naturally deformed rocks (e.g. Rutter et al., 1986; Evans, 1988, 1990; Chester et al., 1993; Evans and Chester, 1995).

Regardless of the complexity of fault rocks, in some

E-mail address: gian@erdw.ethz.ch (G. Manatschal)

0191-8141/99/$ - see front matter
PII: S0191-8141(99)00069-3

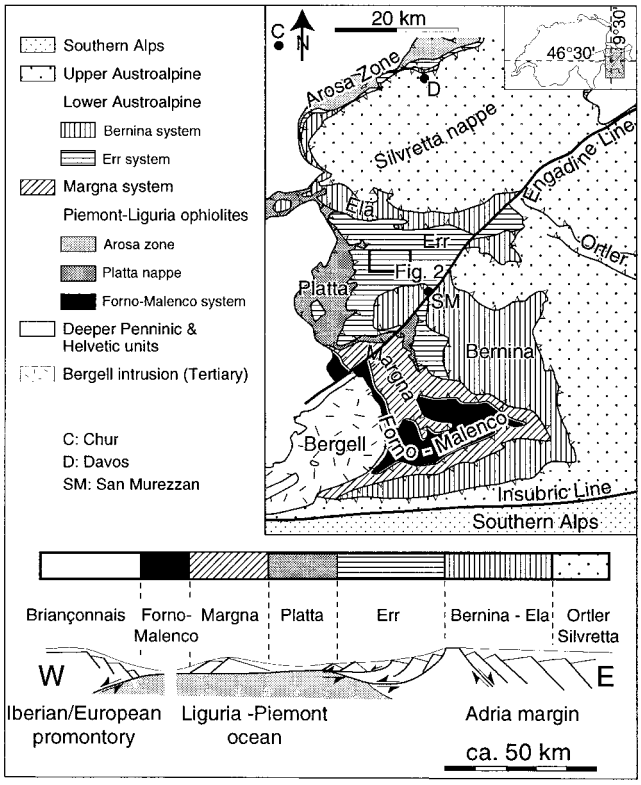

Fig. 1. Tectonic map of the Austroalpine and underlying upper Penninic nappes in eastern Switzerland (above), and an east–west directed palinspastic cross-section across the south Pennine–Austroalpine continent–ocean transition (below) (modified after Froitzheim et al., 1994).

examples, the genesis of the fault rocks and consequently also the conditions during deformation can be deciphered. The fault rocks described in this paper formed along a rift-related low-angle detachment fault in a brittle quartzo-feldspatic upper crust. Strain localization in an advanced stage of faulting within one single, continuous, narrow gouge zone in the center of the detachment resulted in clear overprinting relationships which are neither found in fault zones where strain hardening occurs, nor in anastomosing fault zones. Strain localization and the resulting zonation of the fault zone, documented by systematic changes in lithology, mineralogy, structure, and fabric across the fault zone, allow us to document the genesis of the fault rocks and to study the interplay between deformation and metamorphic reactions in the presence of fluids. This study illustrates that fluid- and reaction-assisted faulting is an important mechanism and may produce very weak fault zones at shallow crustal levels in continental crust.

This paper focuses on the relationship between deformation and mineral reactions whereas the results of a geochemical study of the fault rocks will be published in an accompanying paper (Manatschal et al., in press).

2. Geological overview

The fault rocks discussed here formed along a rift-related low-angle detachment system, today exposed in the Err Nappe in eastern Switzerland (Fig. 1). This detachment system was linked to the opening of the Piemont–Ligurian Tethys Ocean (Froitzheim and Eberli, 1990; Manatschal, 1995; Froitzheim and Manatschal, 1996; Manatschal and Nievergelt, 1997). During Late Cretaceous west-directed nappe-stacking, occurring under lowermost greenschist facies conditions, this rifted margin was incorporated in the South Penninic–Austroalpine nappe pile (Handy et al., 1993; Froitzheim et al., 1994). Within the Err Nappe (Fig. 1), remnants of the low-angle detachment system are spectacularly exposed, as for example in the Piz d'Err–Piz Bial area (Fig. 2). In this area the primary geometry of the detachment system is still preserved. Due to the excellent outcrops in the continent-derived Err Nappe and in the ophiolitic Platta Nappe, the overall geometry of the detachment system, including its relationships to Middle Jurassic syn-rift sediments, could be reconstructed over a distance of at least 35 km parallel to the transport direction (Manatschal and Nievergelt, 1997).

The detachment system comprises at least two low-angle detachment faults which were active in the upper crust over the entire observed length (Fig. 2). This is indicated by the break-down reactions of feldspar to phyllosilicates and by the subordinate importance of crystal–plastic textures in quartz, suggesting that temperatures during faulting did not exceed 300°C. The original low-angle orientation of the detachment faults is confirmed by the absence of a noticeable change in the metamorphism in the footwall rocks over 18 km parallel to the transport direction and by the observed low angle between bedding in the syn-rift sediments onlapping the detachment, and the detachment fault plane (Manatschal and Nievergelt, 1997). The minimum amount of displacement along the low-angle detachment fault is interpreted from the 11 km offset parallel to the transport direction of a characteristic and unique small intrusive body. The sense of displacement of the intrusive body is in line with the top-to-the-west transport direction of the hanging wall as determined by asymmetric clasts, *S–C* fabrics and shear bands (Fig. 2).

3. Fault rocks associated with the low-angle detachment fault

3.1. General

Outcrops preserving relics of the rift-related detachment faults in the Err Nappe are characterized by

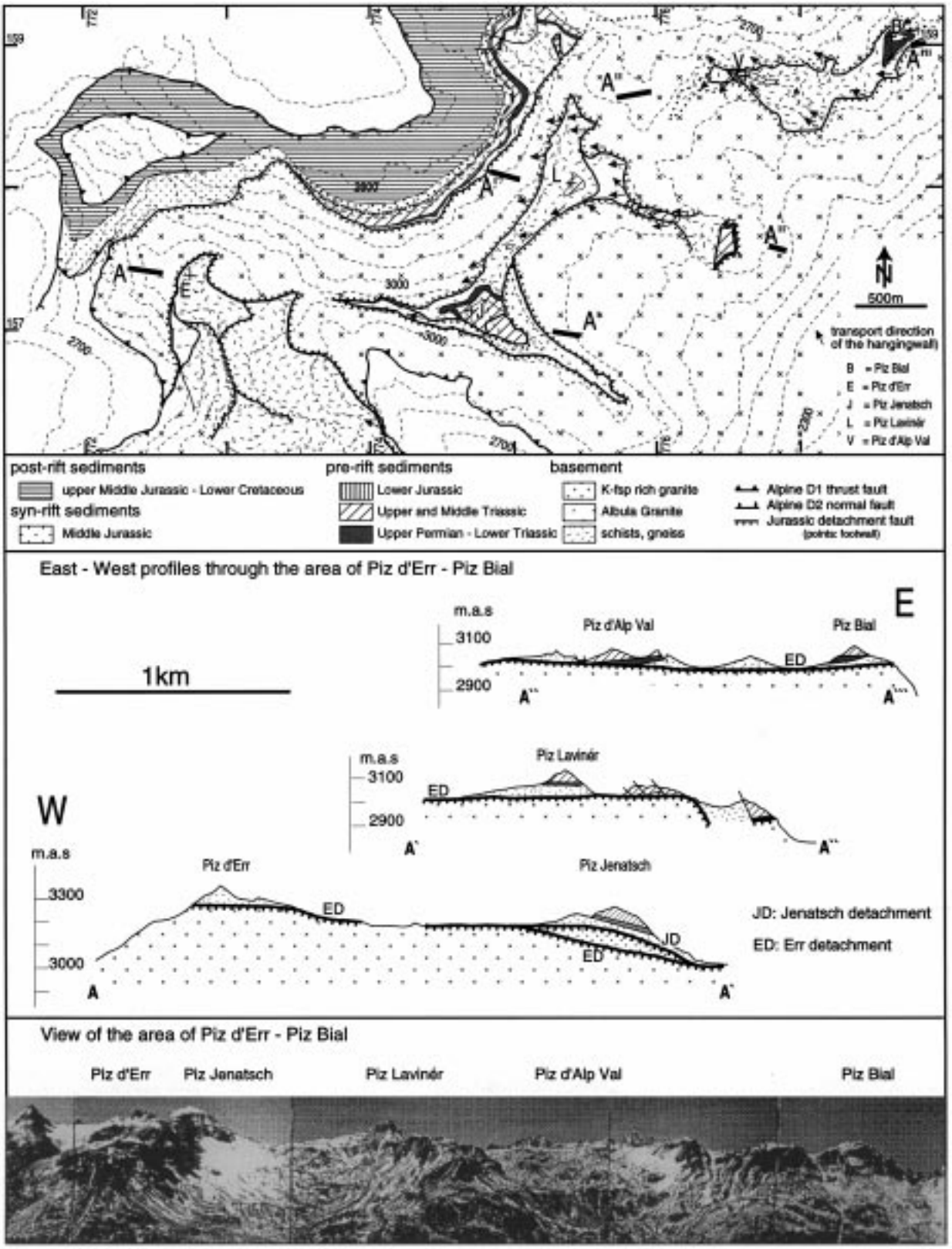

Fig. 2. Geological map of the Piz d'Err–Piz Bial area, where the rift-related detachment system is well exposed and not reactivated by later Alpine deformation (above) (modified after Manatschal and Nievergelt, 1997). For location of the map see Fig. 1. East–west profiles (middle) and view (below) of the detachment system as exposed in the Piz d'Err–Piz Bial area. The distance between Piz d'Err and Piz Bial is about 6 km. For trace of the profile see map (above). Note that the view is oblique to the strike of the profile.

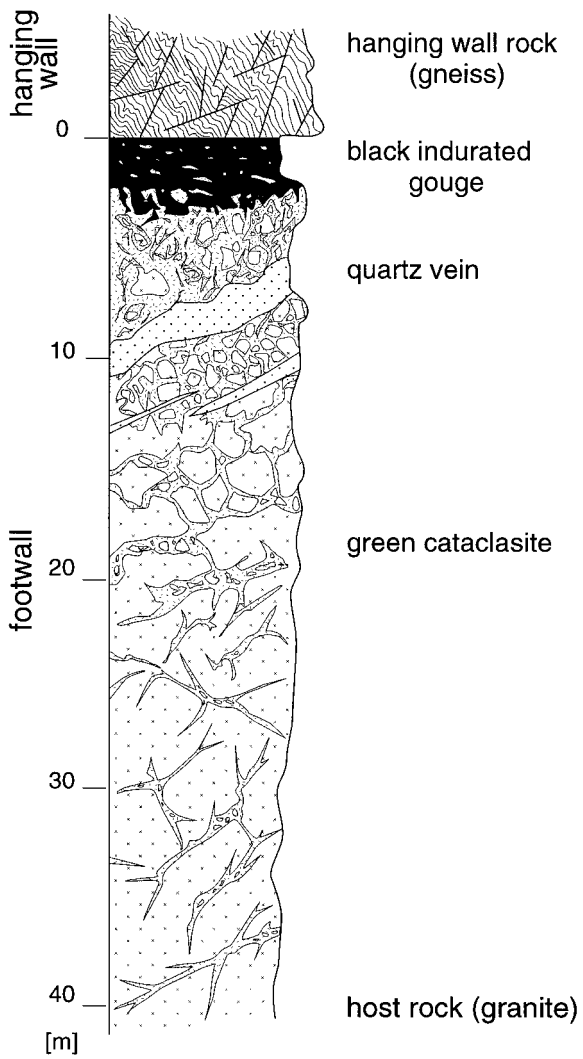

Fig. 3. Schematic profile across a Jurassic detachment fault in the Err Nappe showing the main lithologies accompanying the low-angle detachment fault. The thicknesses of the lithologies in the profile are average values, since the real thicknesses change considerably along strike.

green and black fault rocks. These fault rocks occur only in the footwall of the detachment faults and are distinctly different from fault rocks accompanying Alpine thrust faults (see below). In the past, the black fault rocks were interpreted either as black Carboniferous conglomerates (Cornelius, 1950), or as Alpine 'Reibungskonglomerate' (='friction conglomerats'; Stöcklin, 1949). The occurrence of clasts of these fault rocks in Jurassic syn-rift sediments indicates that their formation obviously predated Alpine orogeny. Therefore and because the detachment faults truncate Triassic dolomites, Froitzheim and Eberli (1990) interpreted them to be related to Jurassic rifting.

Mineralogical composition, fabrics, and structures of the fault rocks accompanying the footwall of the detachment faults in the Err Nappe are very consistent along strike but change considerably across the fault zone, leading to a characteristic zonation of the fault zone. Based on mineralogical composition, fabrics, and structures, four rock types can be distinguished in the footwall of the detachment faults: (1) a host rock which is for the considered area always a Variscan granite; (2) a green cataclasite; (3) a black indurated gouge; and (4) quartz veins (Fig. 3).

The term 'green cataclasite' describes green, cataclasitically deformed granites which show, towards the hanging wall, a transition from a grain-supported to a matrix-supported fabric. The term 'black indurated gouge' is used for a black, well foliated, matrix-supported gouge with less than 30% fragments; 'indurated' implies that the cohesion of the rock results from post-kinematic lithification (for discussion see below).

The hanging wall rocks are, in contrast to the footwall rocks, lithologically and structurally very complex. Deformation in the hanging wall is accommodated by high- and low-angle normal faults which affected the orthogneisses, schists, Permian volcanics and Triassic dolomites (Fig. 2). In contrast to the footwall, syn-kinematic mineral reactions are of subordinate importance in the hanging wall. Although the rocks are intensely faulted, their primary characteristics are still preserved and fault rocks comparable to those occurring in the footwall do not exist in the hanging wall. This paper deals exclusively with the fault rocks occurring in the footwall.

3.2. Host rock

Within the study area, the footwall is composed of late to post-Variscan granite (Albula Granite of Cornelius, 1935). The granite is generally homogeneous and undeformed (Fig. 4a), containing 40–60% plagioclase, 10–30% K-feldspar, 25–45% quartz, and 5–10% biotite and amphibole (Fig. 4b). The plagioclase is altered to sericite, prehnite, pumpellyite, epidote, clinozoisite, albite, and calcite. The K-feldspar is fresh and shows microcline twinning; amphibole is rare. The replacement of biotite by chlorite pre-dates the brittle overprint. Accessory minerals such as apatite, zircon, sphene, allanite, and orthite are commonly associated with the chloritized biotite. The granite does not show evidence of significant pre- or post-detachment deformation, except for a localized Alpine thrust fault south of Piz Jenatsch (Fig. 2).

3.3. Green cataclasite

3.3.1. Fabrics

The transition from the apparently undeformed granite to the green cataclasite is gradational and occurs over a distance of several meters to some tens

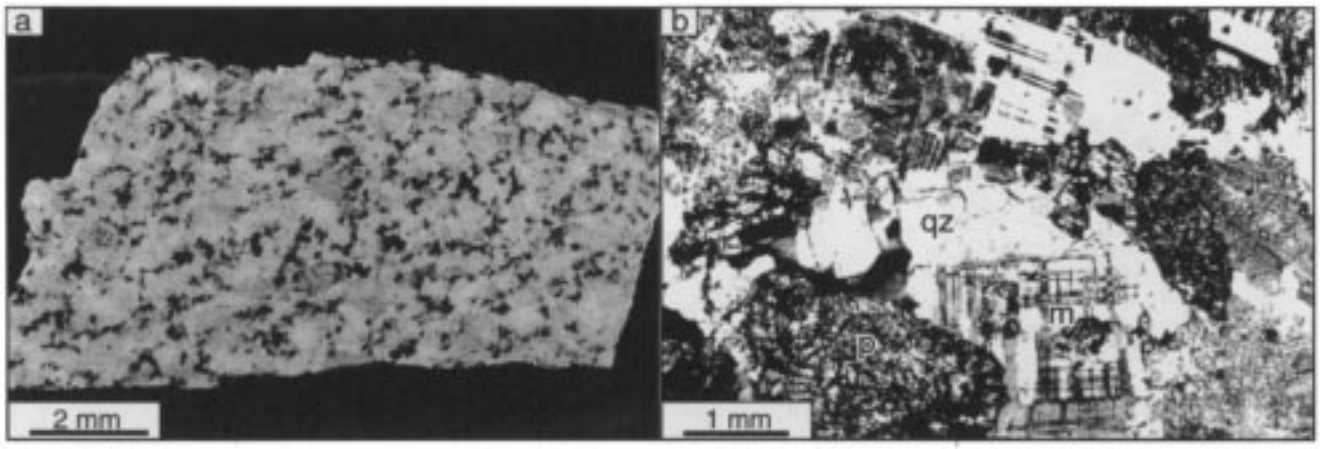

Fig. 4. The host rock in the footwall: (a) Weakly deformed granite from Piz Val Lunga, polished surface (773.7/161.9, 3078 m.a.s.). (b) Thin-section photomicrograph of the sample presented in (a) showing quartz (qz), saussuritized plagioclase (p) and fresh K-feldspar with microcline twinning (m).

of meters. Evidence for brittle deformation within the massive granite is the occurrence of a random network of veins with no consistent overprinting relationships between single sets of veins (Fig. 5a). Commonly, the veins branch with angles between 30° and 45°, form acute angles towards their tip and continue as microcracks in the host rock or crystal (Fig. 5b). Most of the veins are transgranular (Fig. 5c), but intragranular veins can also be observed (Fig. 5b). Microcracks in quartz (Fig. 5b and c) typically terminate at the walls of the veins and do not necessarily continue on the other side of the vein. Typical structures found in this part of the profile are jigsaw-type clasts (Fig. 5c).

Towards the main detachment surface, the veins become interconnected and deformation starts localizing within veins parallel to the surface of the detachment fault. The veins and small-scale fault zones become more dominant, overprint the previously formed network of veins (Fig. 5d) and can be traced over several decimeters or even meters. Increasing veining and faulting lead from a 'vein-in-host-rock' fabric to a breccia fabric where clasts of host rock are surrounded by a matrix of vein material. In zones where deformation localized, the matrix to clast ratio is usually higher than outside these zones (Fig. 5d and e). The matrix is composed of fine-grained angular clasts, the products of cataclasis, and of newly crystallized minerals which are the products of alteration reactions. The clasts are exclusively derived from the granitic host rock.

Towards the main detachment surface, the matrix to clast ratio continuously increases leading to a matrix-supported fabric. This change is usually associated with less angular clasts (Fig. 5f and g), and the appearance of a weak foliation. Already fractured rocks form composite clasts with a fine-grained matrix (Fig. 5h). Up to three episodes of alternate fracturing and healing occur.

3.3.2. Mineralogy

The mineralogical composition of the green cataclasite has been determined by optical microscopy and X-ray diffraction analysis (XRD). In the green cataclasite, primary minerals derived from the granitic host rock, such as quartz, K-feldspar, sericitized plagioclase, and chloritized biotite can be distinguished from secondary, newly crystallized minerals such as illite, chlorite, albite, quartz, calcite, and epidote. Typically, veins are filled with newly crystallized, fine-grained, green-colored minerals. A comparison of the mineral composition of different generations of vein infills indicates a gradual increase in the proportion of phyllosilicates with respect to previously formed matrix. This is well demonstrated in Fig. 5(h), where the later formed matrix ($=M_{II}$) appears darker than the earlier formed matrix ($=M_{I}$) (the darker the matrix the higher the proportion of phyllosilicates). Whereas the primary minerals are strongly affected by microcracks, the newly crystallized minerals commonly do not show any evidence of deformation.

Quartz occurs in the green cataclasite as: (1) angular clasts larger than 50 μm forming, together with feldspar, a load-bearing framework intersected by intra- and transgranular cracks and veins (Fig. 5b and c); (2) rounded clasts (Fig. 5h), generally larger than 50 μm, embedded in a phyllosilicate-rich matrix; and (3) fine-grained (<50 μm) recrystallized aggregates forming, together with albite and phyllosilicates, the matrix. Common micro-structures in the quartz are microcracks and fractures. Deformation bands and lamellae and undulose extinction also occur. Subgrains and lobate grain boundaries were not observed.

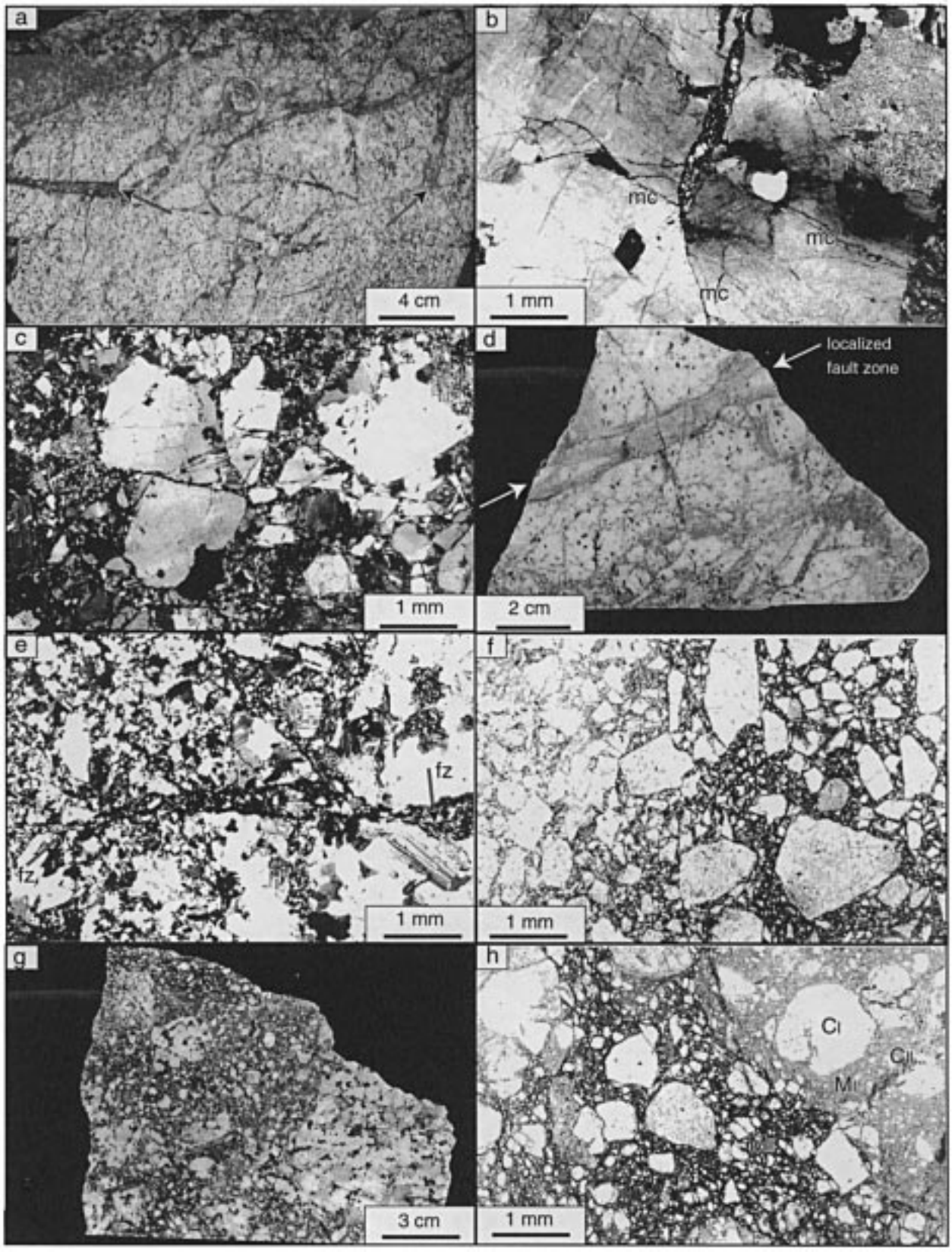

Fig. 5. (*caption opposite*).

The amount of K-feldspar generally decreases with increasing cataclasis across the fault zone. Crushed grains are angular and exhibit a wide range of sizes. Back-scattered-electron images of K-feldspar show curved grain boundaries at contacts with polygonal albite with a uniform grain size of 5–10 μm (Fig. 6a) (cf. Fitz Gerald and Stünitz, 1993). Microprobe analysis across subgrains in K-feldspar shows that the host is composed of almost pure orthoclase (< 1 wt% Na_2O) whereas the newly crystallized subgrains consist of almost pure albite (< 1 wt% K_2O), some also of quartz (Fig. 6b). This suggests a complete exchange of K^+ by Na^+ along sharply defined reaction fronts. In back-scattered-electron images, microcracks are seen in K-feldspar but have not been observed in the albite neoblasts, although albite neoblasts preferentially occur in the prolongation of microcracks in the K-feldspar (Fig. 6a), suggesting a direct relationship between their formation and albitization of the K-feldspar.

Plagioclase is strongly altered in the undeformed granite as indicated by the homogeneous distribution of phyllosilicate and epidote in the cores of plagioclase (Fig. 4b). In the green cataclasite, additionally, phyllosilicates formed along grain boundaries of the plagioclase (Fig. 6c, zone A). With an increasing amount of phyllosilicates a connected network with a strong preferred orientation developed in a matrix-supported fabric (Fig. 6c, zone B).

Finally, calcite occurs in segregation bands within albite and K-feldspar and in veins cutting across localized, phyllosilicate-rich shear zones. Epidote is rare in the green cataclasites. It is mainly found as a fine-grained alteration product in saussuritized plagioclase. At places, veins filled by epidote and quartz can be observed.

3.4. Black indurated gouge

3.4.1. Field observations

The black indurated gouge forms an almost continuous layer with variable thickness, ranging from a few centimeters to some meters in the core of the fault zone. The gouge separates cataclastically, weakly deformed gneiss, schist, and dolomite in the hanging wall from the green cataclasite in the footwall. The contact between the black indurated gouge and the green cataclasite is always sharp (Fig. 7) and locally characterized by injection structures of black gouge into the green cataclasite (Fig. 7a). The injection structures are tapered and joints often occur at their prolongations (Fig. 7b and c).

3.4.2. Fabrics

The black indurated gouge is characterized by a matrix-supported fabric with a clast-to-matrix ratio between 1:10 and 1:3. Regardless of whether the fabric and the grain size distribution are imaged on a decimeter or on a micrometer scale, they always look the same (Fig. 8a–c), suggesting a scale independent fabric- and clast-size distribution in the black indurated gouge. Within the matrix, platy minerals (Fig. 8d and e) and elongated fragments (Fig. 8f) show a strong preferred orientation. The shape of the clasts varies between isometric and elongated lens-shaped. Isometric clasts are commonly well rounded (Fig. 8b). Their sizes range from 1 μm (Fig. 8e) to several cm or even dm (Fig. 8a). Elongated lens-shaped fragments are usually rock types that have a strong pre-existing textural anisotropy such as gneiss or schist. The elongated clasts are always oriented parallel to the main fault plane and range from a few micrometers to some meters across.

In the gouge, σ-type clasts (Fig. 8g) and rarely also δ-type clasts occur and show a top-to-the west sense of shear. *S–C* type fabrics (Fig. 8f and g) with the slip plane parallel to the fault-zone boundary (cf. Berthé et al., 1979) are common, whereas shear-bands with the slip plane oblique to the fault-zone boundary are rare. In electron microscope photomicrographs homogeneous bands consisting of illite and chlorite occur (Fig. 8c and e) and are parallel to the fault-zone boundary. Occasionally, lighter bands composed of

Fig. 5. Fabrics in the green cataclasite: (a) Network of randomly oriented veins overprints the granite. Note characteristic 30–45° angles between branching veins and their sudden termination (arrows). Piz Val Lunga (773.7/161.9, 3078 m.a.s.). (b) Vein within a quartz crystal, filled with fine-grained, newly crystallized, retrograde mineral phases. Microcracks (mc) within the quartz either terminate along the walls at high angle or form the continuation of the veins into the host mineral. Piz Val Lunga (773.7/161.9, 3078 m.a.s.). (c) Cataclastically deformed quartz showing angular clasts, transgranular fractures, and microcracks. The matrix consists of strongly milled host rocks and newly crystallized retrograde phyllosilicates, quartz, and albite neoblasts < 50 μm. Piz Bial (777.7/158.9, 2950 m.a.s.). (d) Localized fault zone (arrows) which is subparallel to the major fault zone, overprints previously formed structures which show a random orientation and are of the same generation as those shown in (a). The localized fault zone is characterized by a higher matrix/clast ratio. Piz Val Lunga (773.7/161.9, 3078 m.a.s.). (e) Thin section photomicrograph showing a fault zone (arrows labelled fz) which initiated in a deformed granite and penetrated the undeformed granite to the right. Piz Val Lunga (773.7/161.9, 3078 m.a.s.). (f) The change from a grain- to a matrix-supported fabric (from the left to the right) is associated with an increase in the proportion of matrix and with a slight decrease in angularity of the clasts. Piz Val Lunga (773.7/161.9, 3078 m.a.s.). (g) Matrix-supported green cataclasite with clasts of undeformed granite embedded in a green matrix. Piz Val Lunga (773.7/161.9, 3078 m.a.s.). (h) Two generations of clasts (C_I and C_{II}) and two generations of matrix (M_I and M_{II}) document successive episodes of cataclasis and subsequent lithification. East of Piz Lavinèr (775.6/157.9, 3000 m.a.s.).

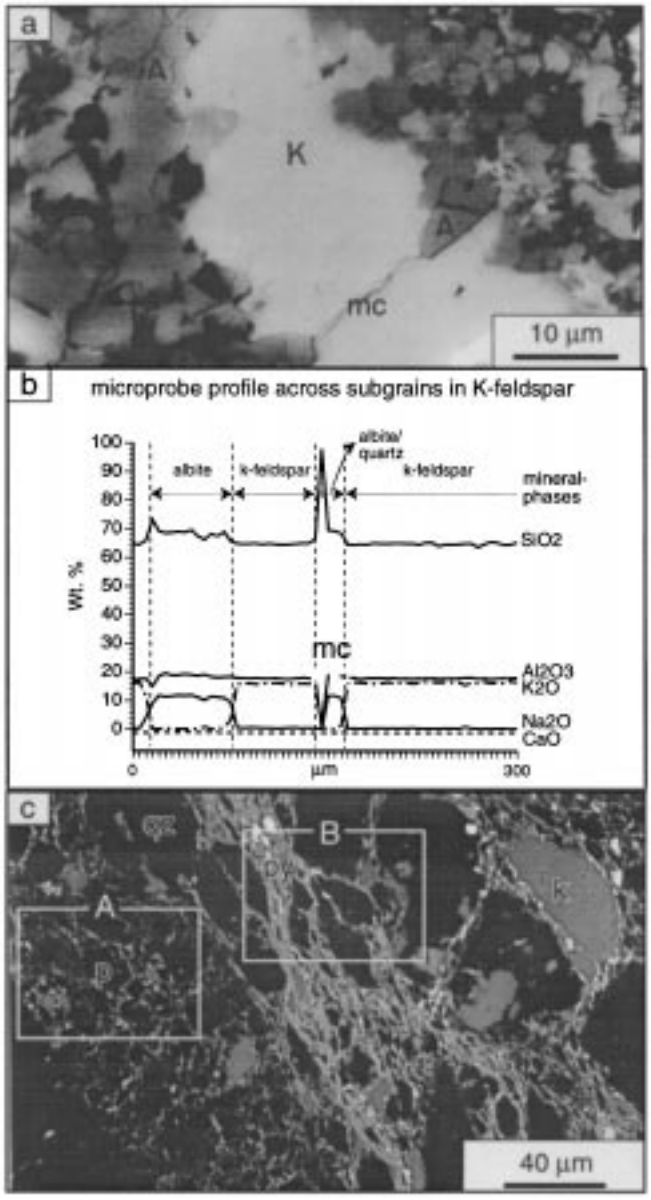

Fig. 6. Mineral reactions occurring in the green cataclasites. (a) SEM back-scattered-electron image of a green cataclasite showing curved grain boundaries of K-feldspar (K), and polygonal albite (A) subgrains (note the 120° triple junctions of the albite subgrains) along the rims. Microcracks in K-feldspar (mc) coincide at their rims with the occurrence of albite subgrains forming an embayment within the K-feldspar. Piz Val Lunga (773.7/161.9, 3078 m.a.s.). (b) Electron microprobe profile across subgrains in K-feldspar. Note the complete replacement of K^+ by Na^+ over a few µm. The profile was made in the sample shown in (a), however, the trace of the profile is outside the illustrated area. (c) SEM back-scattered-electron image of a green cataclasite showing two areas with contrasting fabrics. In the area labelled (A), new crystallization of phyllosilicates is limited to the margins of 'old' plagioclase (p) leading to dispersed phyllosilicates in a grain-supported fabric. In the area labelled with (B), the newly crystallized phyllosilicates (py) form a connected framework with a strong preferred orientation containing partly rounded clasts of K-feldspar (k) and quartz (qz) and with a matrix-supported fabric. Piz Lavinèr (775.6/157.9, 3000 m.a.s.).

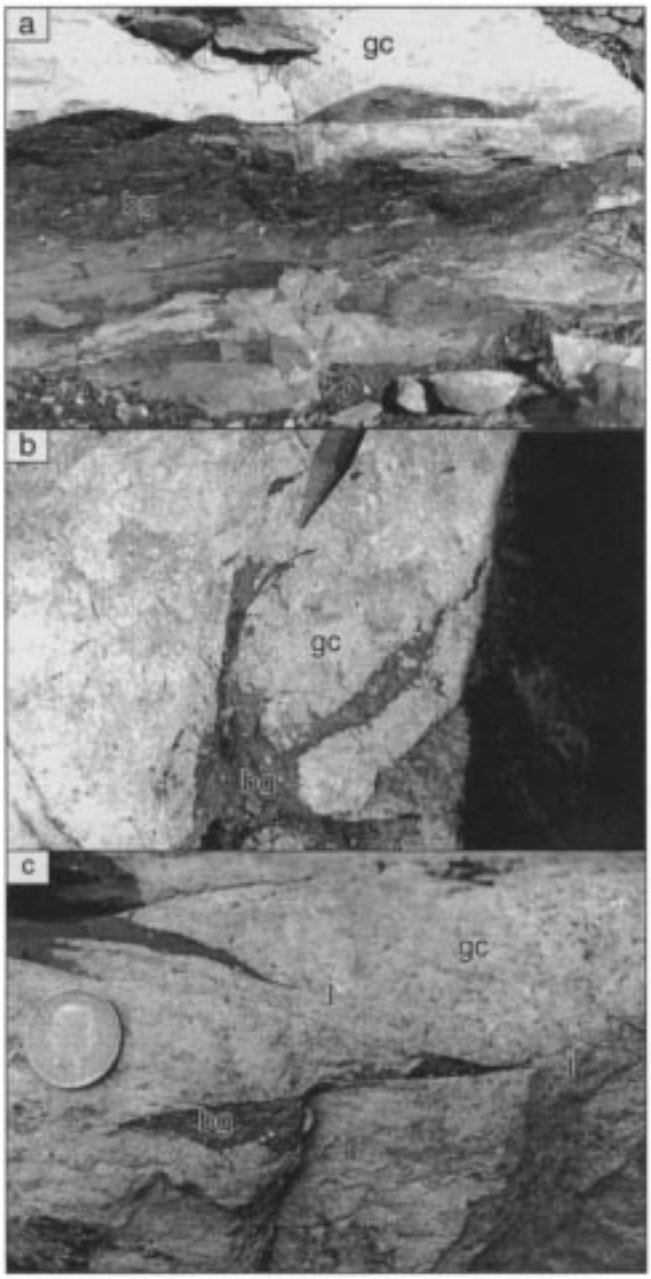

Fig. 7. Contact between the black indurated gouge and the green cataclasite. All examples come from the area south of Piz d'Alp Val (776.8/158.4, 2820 m.a.s.) (Fig. 2). (a) Black indurated gouge (bg) injected into green cataclasite (gc). For scale see pencil just below the label (bg). (b) Detail of the injection structure (pencil for scale). (c) Injection structure in the green cataclasite filled with black indurated gouge (bg). The injections wedge out at a low angle towards the tip and go over into joints (j) in their prolongation.

phyllosilicates mixed with cataclastically deformed material mimic ductile folds (Fig. 8h).

3.4.3. Mineralogy

The mineral composition of the black indurated gouge can be subdivided, similar to the green cataclasite, into primary minerals mainly occurring as clasts

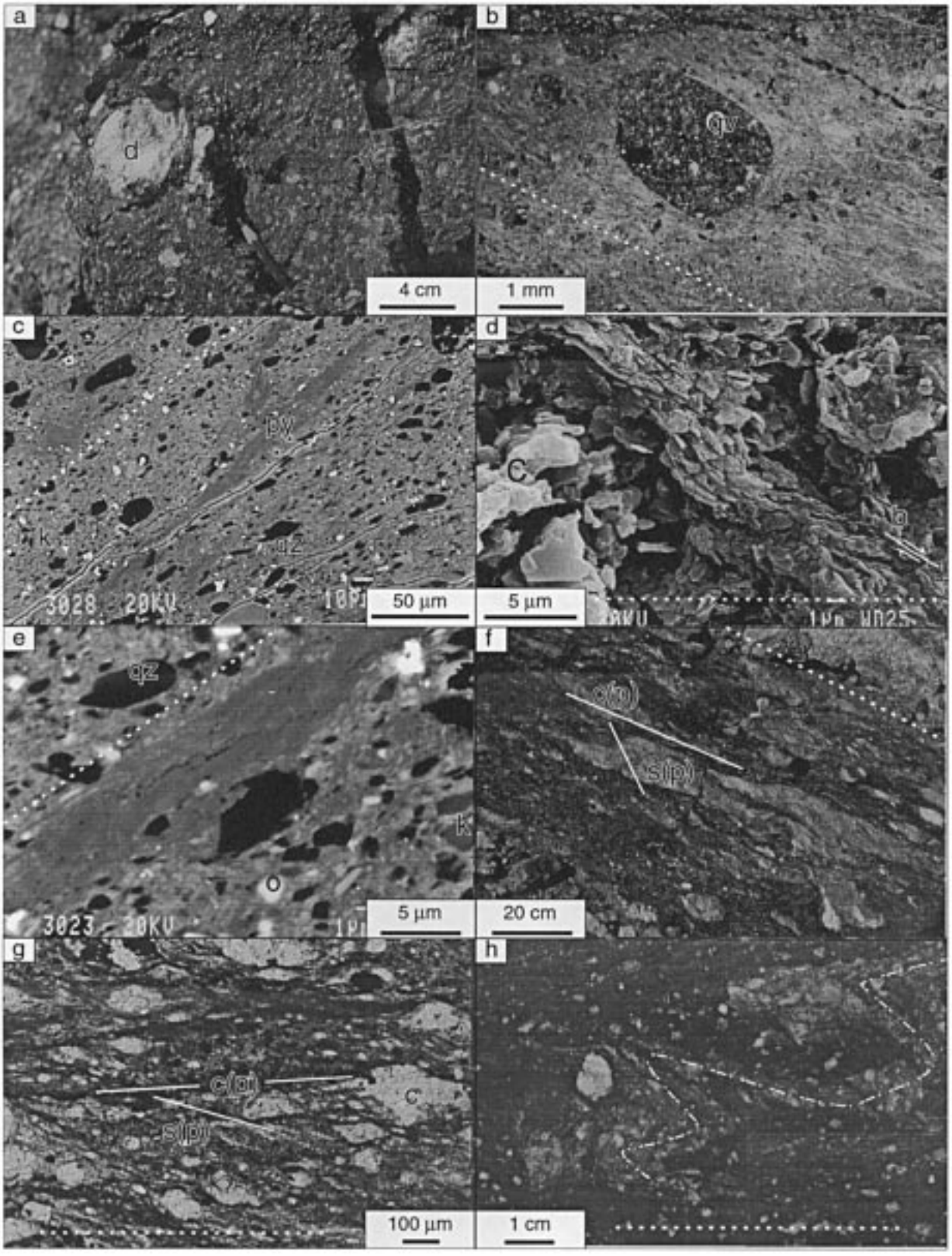

Fig. 8. (*caption overleaf*).

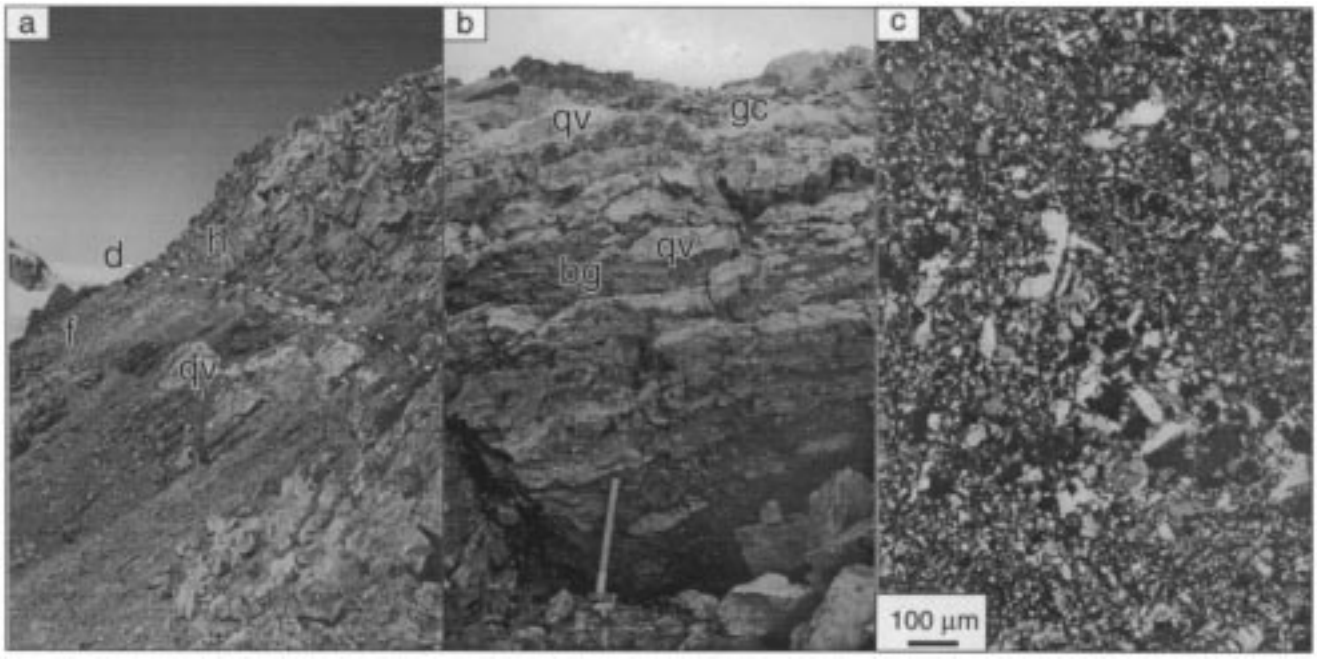

Fig. 9. Quartz veins associated with the low-angle detachment system: (a) A sharp detachment fault (d) separates cataclastically deformed rocks in the footwall (f) from massive gneisses in the hanging wall (h) in the southern face of Piz Jenatsch (see map in Fig. 2). The quartz vein (qv) is about 30 m long, slightly oblique to the detachment surface, and is truncated by the detachment plane. (b) Reworked fragments of quartz veins (qv) together with green cataclasite (gc) embedded in the black indurated gouge (bg). North of the summit of Piz Val Lunga (773.6/162.2, 2869 m.a.s.). Hammer for scale. (c) Thin section photomicrograph showing recrystallized quartz and lesser albite. Grain size ranges from 100 µm to a few µm. Southwest face of Piz Bial (777.7/158.9, 2950 m.a.s.).

and newly crystallized minerals forming the matrix. The transition from the green cataclasite to the black indurated gouge is defined by a change in the relative abundance of feldspar and phyllosilicates and not by the occurrence of new mineral phases, except for graphite. The relative amount of feldspar in the green cataclasite is between 40 and 70%; in the black indurated gouge it is below 10%. The relative amount of phyllosilicates in the green cataclasite is between 10 and 40% and increases to more than 60% in the black indurated gouge.

The composition of the matrix, i.e. the fraction < 2 µm, was determined by X-ray diffraction analysis (XRD) and Fourier transform infrared spectroscopy (FT-IR). It consists of chlorite, illite, quartz, and subordinate albite. Chlorite and illite form intergrown aggregates. The carbon content of the fraction < 2 µm was determined to be between 2 and 6 wt%. The occurrence of graphite may cause the black color of the gouge. Under the microscope, syn- as well as post-kinematic calcite was observed. Epidote was not observed in the matrix.

Fig. 8. Fabrics, structures, and mineral composition of the black indurated gouge. Dotted white lines indicate the orientation of the detachment fault boundary. (a) Rounded Triassic dolomite clast (d) within black indurated gouge at Cuotschens (774.05/162.60, 2850 m.a.s.). (b) Thin section photomicrograph of a black indurated gouge showing a perfectly rounded clast derived from a quartz vein (qv), embedded in a phyllosilicate-rich matrix with a strong preferred orientation. 'Mulixer Keil' (775.6/161.4, 2440 m.a.s.). (c) SEM back-scattered-electron image showing a strong preferred orientation defined by elongated clasts of quartz (qz), K-feldspar (k), and bands consisting of pure phyllosilicate (py). The orientation of the foliation is subparallel to the orientation of the fault zone. South of Piz d'Alp Val (776.8/158.4, 2820 m.a.s.). (d) SEM image of a leached (with HCl) black indurated gouge showing orientation and grain size of the phyllosilicates in the pressure shadow of a clast (c) (now forming a negative relief due to leaching). Shear band like structures occur in the tail of the asymmetric clast (b). Piz Val Lunga (773.6/162.2, 2869 m.a.s.). (e) SEM back-scattered-electron image showing the black indurated gouge at a high magnification. Many clasts of quartz (qz), K-feldspar (k), and opaque minerals (o) are below 5 µm and are embedded in an extremely fine-grained matrix consisting of intergrown chlorite and illite. Bands consisting exclusively of phyllosilicates are parallel to the preferred orientation of the elongated clasts. South of Piz d'Alp Val (776.8/158.4, 2820 m.a.s.). (f) Elongated, lens-like fragments of a foliated cataclasite in the black indurated gouge. Fault zone-parallel fault planes initiate along the elongated rims of the fragments [C(p)]; foliation within the clasts [S(p)] is oriented at an angle of about 30° to the fault plane. This S–C-type geometry suggests a sinistral sense of shear. From these and similar structures (g), a top to the west movement direction was determined (see transport directions in the map in Fig. 2). Outcrop south of Piz d'Alp Val (776.8/158.4, 2820 m.a.s.). (g) Thin-section photomicrograph of a black indurated gouge showing S–C fabrics [S(p) and C(p)] and asymmetric clasts (C) both indicating a sinistral sense of shear. Val Rudé (796.5/163.04, 2480 m.a.s.). (h) Ductile folds in a black indurated gouge. Fuorcla Mulix (775.3/158.9, 2880 m.a.s.). Dotted line indicates the shape of the folds.

Table 1
Comparison between the green cataclasite and the black indurated gouge

	Green cataclasite	Black indurated gouge
Metamorphic conditions during deformation	< 300°C	< 300°C to surface conditions
Accommodated strain	low to moderate, mainly in-situ brecciation	very high displacement (> 11 km)
Fabric	highly variable: ranging from jigsaw-type fabrics to grain- and matrix-supported fabrics	very homogeneous: matrix-supported fabric
Structures	Intra- and transgranular fractures, microcracks, angular clasts	strong shape preferred orientation, *S–C* structures, shear bands, ductile folds, injection structures, rounded or lens-shaped clasts
Rheologically dominant mineral phase	quartz and feldspar	phyllosilicates
General nature of deformation	brittle and dilatant	ductile (on a macroscopic scale)
Cohesion at time of deformation	repeated failure events followed by healing	no cohesion as indicated by injections into the neighboring rocks
Deformation mechanisms and retrograde break-down reactions	cataclasis and simultaneous break-down reactions of feldspar leading to the formation of phyllosilicates	controlling deformation mechanism not directly discernible; suggested process is grain boundary sliding; cataclasis is of subordinate importance
Availability of fluid, permeability	presence of fluid in a highly permeable fault system	presence of fluid in a fault zone with a bulk anisotropic permeability

The mineralogical composition of the matrix is very homogeneous throughout the studied area. In contrast, the composition of the clasts is more local and clasts deriving from the footwall are more frequent than those deriving from the hanging wall. Clasts of undeformed granite have not been found so far in the black indurated gouge which is compatible with the observation that the gouge is always separated from the granite by the green cataclasite. The composition of the clasts depends on their size. With decreasing size, polymineralic litho-clasts become less abundant and are successively replaced by monomineralic clasts. Monomineralic clasts consist mainly of quartz and remnants of feldspar, and to a lesser extent also of apatite, zircon, garnet, mica, and chloritized biotite. Sphene, pyrite and other opaque minerals are commonly associated with localized shear zones, but occur also as rounded clasts in the matrix.

3.5. Quartz veins

Light-colored, slightly discordant quartz veins, up to 2 m wide and several tens of meters long (Fig. 9a), are associated with the fault rocks. These quartz veins are restricted to the cataclastically deformed zone in the footwall of the low-angle detachment faults and have not been found so far in the hanging wall. The quartz veins systematically cut across small-scale structures in the green cataclasite but cross-cut no structures in the gouge. Fragments of quartz veins commonly occur as rounded or lens-shaped clasts in the gouge (Fig. 9b). Under the microscope, the quartz veins show cataclastically deformed fragments surrounded by microcrystalline quartz and albite (Fig. 9c). X-ray fluorescence analysis (XRF) of quartz veins yielded values ranging between 88 and 96 wt% SiO_2, confirming the dominance of quartz over albite.

3.6. Overprinting relationships between the different fault rocks

Two generations of systematic overprinting relationships can be recognized between the different rock types described above. A first generation is well preserved along the margins of the fault zone and characterized by small-scale localized brittle fault zones which are parallel to the main fault zone and overprint a network of veins (Fig. 5d). A second generation is preserved in the core of the fault zone where injections of black indurated gouge into the green cataclasite (Fig. 7a–c) and clasts of green cataclasite in the gouge clearly document that deformation in the gouge outlasted deformation in the green cataclasite.

The two generations of overprinting relationships indicate a shift in fault activity towards the center of the fault zone, suggesting that deformation initiated within

a wide band and localized afterwards within a narrow, weak zone which accommodated most of the displacement. This is also supported by the cross-cutting relationships between the quartz veins and the fault rocks. The quartz veins cut across internal structures in the green cataclasite; they are in turn truncated by the main fault plane (Fig. 9a); and clasts derived from them occur in the black indurated gouge (Fig. 9b).

4. Comparison with fault rocks from Alpine thrust faults

Fault rocks, similar to the black indurated gouge, are commonly described from extensional detachment and wrench faults but have not been described from thrust fault systems. In the studied area a comparison between fault rocks from Alpine thrust faults and Mesozoic extensional detachment faults is possible. Both fault types overprint the same granite at lower greenschist facies or even lower metamorphic conditions, and the displacement is in both cases on a kilometer scale.

Quartz microstructures within the fault rocks of the two fault zones are similar and dominated by fractures, microcracks, undulose extinction, deformation bands and deformation lamellae. Nucleation of subgrains or evidence for grain boundary migration were not found. In contrast to the quartz microstructures, the overall structures and fabrics of the fault rocks are different. The thrust-related fault rocks do not show a zonation of different fault rock lithologies, instead they are dominated by *S–C* fabrics and shear bands in a grain-supported framework. A major difference between the low-angle extensional and thrust related fault rocks appears to be the intensity of syn-kinematic crystallization of phyllosilicates which is excessive in the former fault rock type.

5. Discussion

The discussion focuses on: (1) the nature of the fault rocks; (2) the interaction between deformation processes and retrograde metamorphic reactions in the presence of fluids; and (3) the genesis of the fault rocks and the related evolution of the fault zone.

5.1. Nature of the fault rocks

5.1.1. Deformation mechanisms

A summary of constraints, observations and inferences on which the following discussion about deformation mechanisms is based, is presented in Table 1.

In the 'green cataclasite' angular clasts, microcracks and fractures indicate that cataclasis, i.e. brittle fracturing, was the controlling deformation process in these rocks. Evidence for other deformation mechanisms active in these rocks is absent.

Determination of the deformation mechanisms operating in the 'black indurated gouge' is hampered, because the microstructural and textural products of some probably active deformation mechanisms are not preserved or were overprinted by later events. Surficially, the black indurated gouge looks similar to pseudotachylites as suggested by the black coloration and the injection of veins with sharp boundaries with the wall rock (Fig. 7). However, pseudotachylite features indicative of a melt origin, such as quenched vein margins (e.g. Philpotts, 1964), vesicles and amygdales (e.g. Maddock et al., 1987), newly crystallized minerals stable only at high temperatures (e.g. Toyoshima, 1990), melting effects preserved in clasts (e.g. Maddock, 1986; Magloughlin and Spray, 1992), spherical coronas and reworked clasts of older pseudotachylites (Sibson, 1975) are absent in the black indurated gouge. Moreover, clasts showing resorption phenomena are missing and the black gouge contains clasts smaller than 5 μm in the matrix (Fig. 8e), a clast size which is almost absent in pseudotachylites (Shimamoto and Nagahama, 1992). All these observations argue against a formation of the 'black indurated gouge' as a pseudotachylite.

Fabric elements in the black gouge such as the strong foliation, *S–C* fabrics, asymmetric clasts, and folds (Fig. 8) are unlikely to result from cataclasis alone and look surprisingly similar to structures occurring in some greenschist facies quartzo-feldspatic mylonites (e.g. Passchier and Trouw, 1996), although the underlying deformation mechanisms are different. Within the black indurated gouge, no evidence for intracrystalline plasticity has been found. The scale-independence of the fabric which is not found in mylonites but is characteristic of cataclasites and gouges (Sammis et al., 1986), suggests that the grain-size distribution is controlled by cataclastic processes, although typical cataclastic structures such as angular clasts and fractures are absent in the black indurated gouge. A possible cataclastic process which may occur in the black indurated gouge is frictional wear of previously brecciated angular clasts (Scholz, 1987). This process would explain the well rounded shape of some of the clasts and the formation of a wear detritus. However, the deformation mechanism controlling the strain accommodation in the gouge must be located in the phyllosilicate-rich matrix, in which the deformation was localized.

In the matrix no evidence for one specific deformation mechanism has been observed. Traces of cataclasis or intracrystalline deformation may be found locally; however, they are clearly of subordinate importance, indicating that another not ascertainable deformation mechanism had to be active as well. A

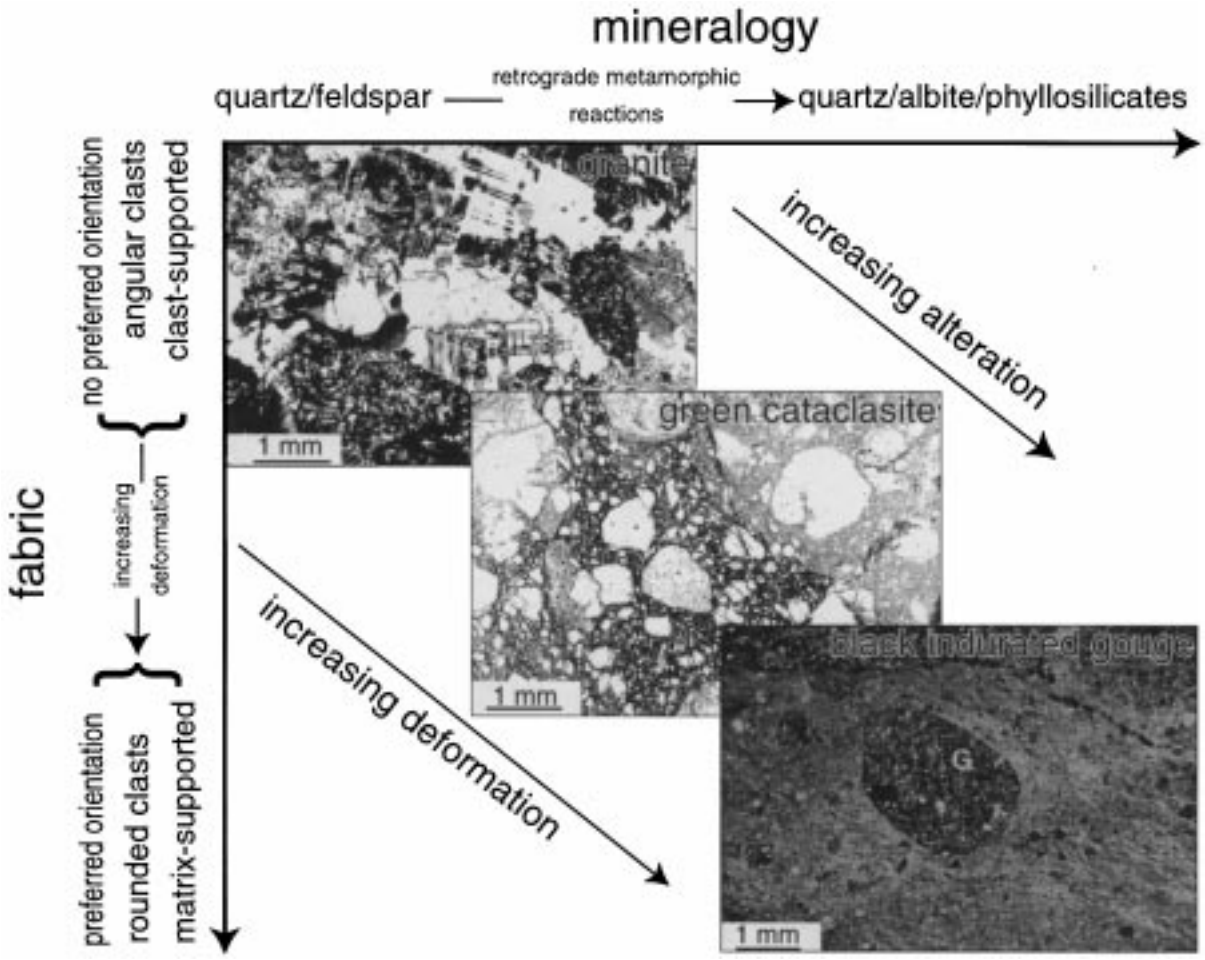

Fig. 10. Phenomenological relationships between mineralogical composition and fault rock fabric observed in rift-related detachment faults.

possible candidate which is, however, difficult to document since it does not leave characteristic traces in the microstructure, is intercrystalline gliding. The strong preferred orientation of the phyllosilicates, the occurrence of pure phyllosilicate bands which are parallel to the main fault plane (Fig. 8c and e), and the ductile style of deformation (the term 'ductile' refers in this work only to processes occurring on a macroscopic scale), are compatible with intercrystalline deformation processes such as grain boundary sliding (e.g. Boullier and Gueguen, 1975).

5.1.2. Classification

The syn-kinematic mineral assemblage, the subordinate importance of intracrystalline deformation in quartz, and the generally brittle nature of the structures associated with the fault rocks indicate that their formation occurred at low temperatures in the brittle field. Published classifications for brittle fault rocks (e.g. Heitzmann, 1985; Rutter, 1986; Groshong, 1988; Schmid and Handy, 1991) commonly use descriptive as well as genetic criteria. As previously mentioned, the determination of genetic criteria such as active deformation mechanisms is difficult; however, the use of descriptive criteria is in some cases not less ambiguous. The terms 'cohesive' and 'incohesive', commonly used to distinguish between cataclasites and gouges, are difficult to use for ancient fault rocks. In a correct genetic classification, the presence or absence of cohesion should be related to the time of active deformation, and not to the present stage. Therefore, to distinguish between gouge and cataclasite additional criteria such as type of structures and fabrics, matrix-to-clast ratio, and shape of clasts should be considered as well.

For the fault rocks discussed here, the cataclastic nature of the green cataclasite is not disputed, and evidence against a pseudotachylitic nature of the black indurated gouge has been discussed above. That the black indurated gouge formed as a non-cohesive gouge and lithified post-kinematically, as proposed by using the term 'indurated gouge', is indicated by the occurrence of injection veins (Fig. 7) as well as by the strong similarity with fault rocks interpreted as fault gouges (cf. Engelder, 1974; Chester and Logan, 1987; Evans and Dresen, 1991). An alternative interpretation, that the black fault rocks retained cohesion during defor-

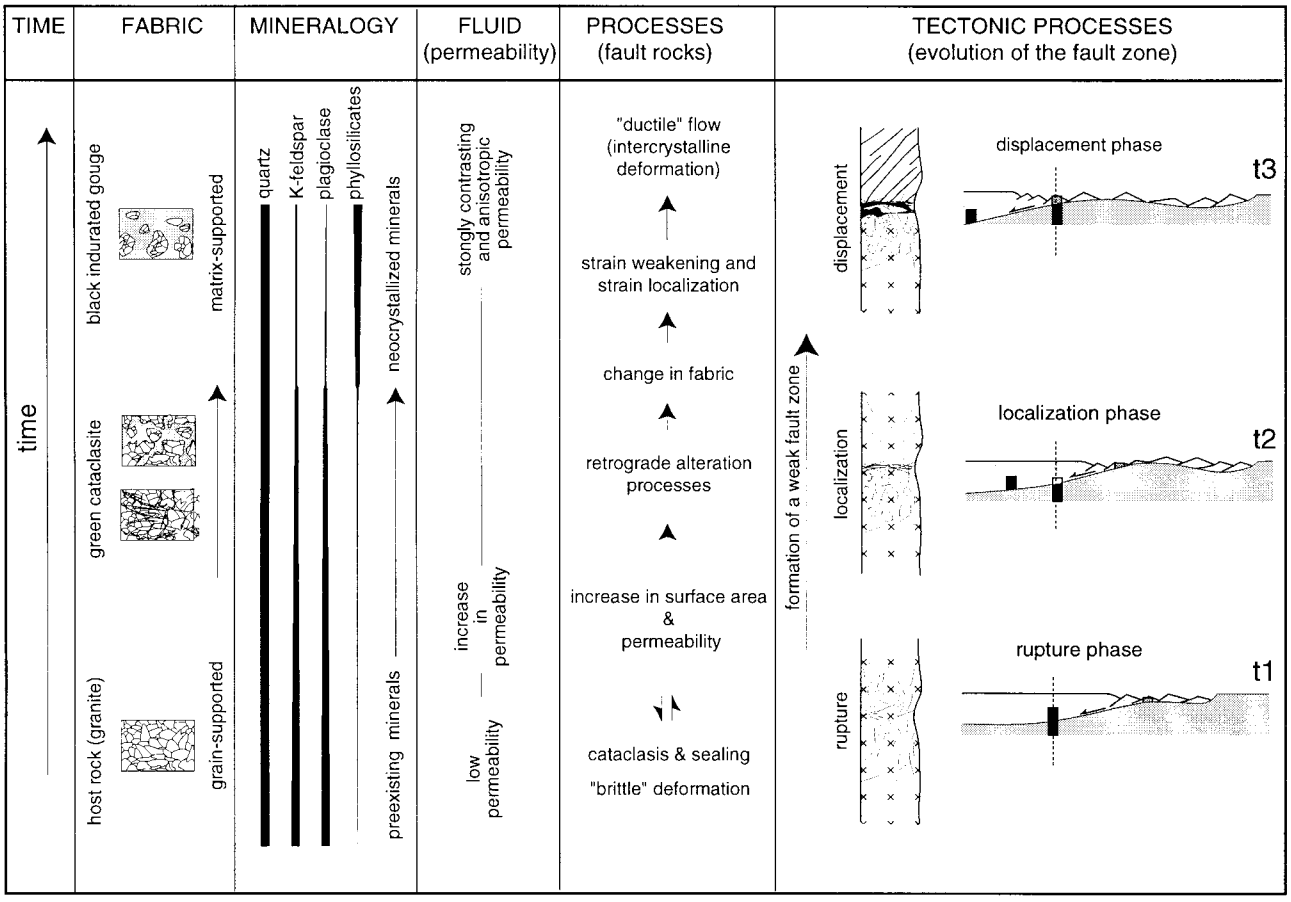

Fig. 11. Genetic model explaining the evolution of fabric, mineralogy, and permeability during low-angle detachment faulting along a rift-related detachment system in the Err and Platta nappes.

mation and formed as foliated cataclasites (Chester et al., 1985) appears to be, based on the available observations, rather unlikely. Since fabrics of cataclasites and gouges look different, and their deformation history and deformation mechanisms are different as well, their distinction is important and should therefore not be based on the occurrence or absence of cohesion alone.

5.2. The role of fluid- and reaction-assisted deformation in the formation of the fault rocks

5.2.1. Evidence for reaction-induced softening

Syn-kinematic, retrograde break-down reactions of feldspar resulting in the neocrystallization of weaker phases such as phyllosilicates, strongly control the strength of fault zones (e.g. Wintsch et al., 1995). The observed increase in the phyllosilicate/feldspar ratio changes the fabric from an initially grain-supported framework to a matrix-supported fabric (Fig. 6c). Such a change in fabric is often associated with a strain softening if the replacing minerals (phyllosilicates) are weaker than the replaced minerals (feldspar) (e.g. Jordan, 1987; Handy, 1990). The effect of strain localization is illustrated in Fig. 6(c) where the change from a grain- to a matrix-supported fabric is associated with the transition from a random to a preferred orientation of the phyllosilicates (Fig. 6c, areas A and B).

5.2.2. Evolution of the fault rocks

The most obvious change in a profile across the low-angle detachment fault is the changing mineralogy and fabric recorded in the transition from the granite across the green cataclasite to the black indurated gouge (Figs. 3 and 10). Changes in mineralogy can be described by break-down reactions of feldspar (plagioclase and K-feldspar) in the presence of fluid under retrograde metamorphic conditions resulting in the crystallization of quartz, albite, phyllosilicates (sericite and chlorite) and calcite. The break-down reactions of feldspar are enhanced by cataclasis resulting in grain-size reduction, increasing surface/volume ratio, and higher permeability.

Fabrics across the fault zone change from a magmatic fabric in the undeformed footwall to a jigsaw-type or clast-supported fabric at the margin of the fault zone which grades over into a matrix-supported

fabric towards the core of the fault zone. In the same direction, also a change in shape from angular to rounded clasts and the development of a strong foliation can be observed (Fig. 10).

The systematic changes in mineralogy and fabric are the finite expression of fault zone development during strain localization. The amount of accommodated strain can be related to changes in mineralogy (=alteration processes) and fabric (=mechanical processes) (Fig. 10). Fault rocks in low strain zones (e.g. green cataclasite), are characterized by a high proportion of unstable primary minerals (e.g. feldspar) and exhibit a clast-supported framework with angular clasts. In contrast, fault rocks in high strain zones (e.g. black indurated gouge) have a high proportion of newly crystallized phyllosilicates and show a matrix-supported fabric with rounded clasts and a strong grain-shape preferred orientation.

5.3. Permeability of the fault zone

Although no permeability measurements exist from the fault rocks described here, Chester and Logan (1986) and Caine et al. (1996) demonstrated for similar fault rock types that the average mean permeability of the gouge zone is expected to be significantly lower than that of the damaged and undeformed host rock. Evans et al. (1997) investigated the permeability of fault-related rocks from a brittle fault zone in granitic rocks, i.e. very similar rocks to the ones described here. Their tests, performed at low confining pressures, indicated that the highest permeabilities were present in the damaged zone (10^{-16}–10^{-14} m^2), that lowest permeabilities occurred in the fault core (10^{-20}–10^{-17} m^2), and intermediate permeabilities were measured in the protolith (10^{-17}–10^{-16} m^2). These results compare well with in-situ measurements of permeability in drill holes (Brace, 1984; Neuzil, 1994) which yield typical values for crystalline rocks ranging between 10^{-18} and 10^{-13} m^2, and for shales, which may be a good equivalent to a clay-rich gouge, ranging between 10^{-20} and 10^{-18} m^2.

Assuming that these results can be applied to the here discussed detachment fault and considering the evolution of the fault rocks, it seems clear that the permeability of the fault zone had to change through time and is strongly controlled by fluid- and reaction-assisted cataclasis. In an initial stage of faulting, the permeability may have increased as a consequence of fracturing. The increasing amount of newly crystallized phyllosilicates during faulting may have resulted in a decrease and strong anisotropy of the permeability in the fault core, as indicated by the measurements of Evans et al. (1997). The strong preferred orientation of the phyllosilicates in the gouge may have amplified the anisotropy of the permeability.

5.4. Evolution of a low-angle detachment fault

The structural and mineralogical evolution of the fault rocks as well as the overprinting relationships demonstrate that deformation in the footwall of the detachment fault localized in the internal parts of the fault zone. Consequently, the fault rocks from the margins of the fault zone are interpreted to record early phases of deformation whereas fault rocks in internal parts of the fault zone preserve the later phases. Thus, the fault rocks occurring along the detachment fault do not only show a strain gradient, but also record a sequence of deformation events. Fig. 11 illustrates these events and the associated changes in fabric, mineralogy, and permeability.

5.4.1. Initiation of deformation: 'rupture phase'

At the margin of the fault zone a network of veins filled with newly crystallized sericite, chlorite, fine-grained albite, quartz, epidote, and calcite overprints the undeformed granite (Fig. 5a). Because of the brittle nature of the deformation and based on the syn-kinematic retrograde mineral assemblage including hydrous mineral phases, this deformation occurred under lower greenschist facies or even lower metamorphic conditions and in the presence of fluid. The lack of a preferred orientation, the branching and sudden termination of veins (Fig. 5a), injection of fine-grained newly crystallized matrix in veins (Fig. 5b), and the jigsaw-type pattern formed by the interleaving undeformed granite (Fig. 5a), suggest that these veins formed as tensile fractures in the presence of a transient high fluid pressure (cf. Reynolds and Lister, 1987). Several cycles of fracturing and healing events are indicated by the occurrence of several generations of cataclasites (Fig. 5h). Repeated failure may have led to pervasive fracturing resulting in a finer grain size with a high surface/volume ratio and a higher permeability, facilitating fluid infiltration and catalyzing the breakdown reactions of feldspar. Thus, in the initial stage of deformation cataclasis and alteration reactions were cogenetic processes and controlled permeability.

5.4.2. Initial localization of deformation: 'localization phase'

Tensile veins with no preferred orientation are generally overprinted by local fault zones which preferentially use preexisting veins arranged parallel to the main fault zone (Fig. 5d). The occurrence of rounded clasts, indicating a rotational component, and the formation of a foliation subparallel to the fault zone suggest shear deformation along these anastomosing fault zones. Shear deformation was probably localized preferentially in zones with a high proportion of phyllosilicates (Fig. 6c) (e.g. Wintsch et al., 1995).

5.4.3. Displacement along a localized shear zone: 'displacement phase'

A large part of the at least 11 km of displacement along the detachment fault was accommodated within the narrow zone represented by the black indurated gouge (Manatschal and Nievergelt, 1997). Assuming a width of about 1 m for this zone, shear strains in excess of several thousands would have been imposed in this shear zone. Thus, the gouge in the fault zone had to be extremely weak and probably acted as a lubricant between hanging wall and footwall rocks. The microstructures in the gouge do not record evidence of particular deformation mechanisms. However, injection structures observed at the margins of the gouge (Fig. 7) may indicate that the generation of transient high-fluid pressure along the detachment was an important process and was able to trigger seismic failure during slip along a transient very weak fault zone (e.g. Miller et al., 1996). Earthquakes along a low-angle detachment fault linked to a non-volcanic rifted margin have been documented recently by Albers et al. (1997) in the Woodlark Basin.

6. Conclusion

Fault rocks sampled along profiles across a rift-related detachment fault in the Err Nappe (Eastern Alps) document deformation processes, metamorphic reactions, fluid flow, and the strain history of the fault zone. Cross-cutting relationships suggest that the deformation history of the fault zone begins with cataclasis, maybe enhanced by transient high fluid pressures in a granitic basement. Dilatation associated with cataclasis led to an increase in the surface/volume ratio of the clasts and to a higher permeability, facilitating fluid mobility and enhancing the alteration of feldspar leading to the crystallization of phyllosilicates. The increasing amount of phyllosilicates is suggested to be the key factor in controlling the strength and permeability of the fault zone. Thus, the interplay between fluid, mineral reactions, and deformation can result in softening processes which can reduce the frictional strength of the fault zone to such an extent that normal faults can slip even at low-angles in the brittle upper crust.

Acknowledgements

I thank Daniel Bernoulli, Niko Froitzheim, Martin Burkhard, and Raymond Franssen for comments, suggestions, and very helpful reviews. I would like to thank Holger Stünitz and Neil Mancktelow for helpful discussions, Rolf Nüesch, Djordje Grujic, Jörg Hermann, and Piotr Gawenda for having provided help in laboratory work, and Eva Sauter for having read the last version of this manuscript. The work published in this paper is part of my PhD thesis and was supported by ETH Zürich research grant 0-20-569-92.

References

Albers, G.A., Mutter, C.Z., Fang, J., 1997. Shallow dips of normal faults during rapid extension: Earthquakes in the Woodlark–D'Entrecasteaux rift system, Papua New Guinea. Journal of Geophysical Research 102, 15301–15317.

Anderson, E.M., 1951. The Dynamics of Faulting, 2nd ed. Oliver & Boyd, Edinburgh.

Berthé, D., Choukroune, P., Jegouzo, P., 1979. Orthogneiss, mylonite and non-coaxial deformation of granites: the example of the South Amorican Shear-Zone. Journal of Structural Geology 1, 31–42.

Boullier, A.M., Gueguen, Y., 1975. SP-Mylonites: Origin of some mylonites by superplastic flow. Contributions to Mineralogy and Petrology 50, 93–104.

Brace, W.F., 1984. Permeability of crystalline rocks: new in situ measurements. Journal of Geophysical Research 89, 4327–4330.

Caine, J.S., Evans, J.P., Forster, C.B., 1996. Fault zone architecture and permeability structure. Geology 24, 1025–1028.

Chester, F.M., Logan, J.M., 1986. Implications for mechanical properties of brittle faults from observations of the Punchbowl fault zone, California. Pure and Applied Geophysics 124, 79–106.

Chester, F.M., Logan, J.M., 1987. Composite planar fabric of gouge from the Punchbowl Fault, California. Journal of Structural Geology 9, 621–634.

Chester, F.M., Friedman, M., Logan, J.M., 1985. Foliated cataclasites. Tectonophysics 11, 139–146.

Chester, J.P., Evans, J.P., Biegel, R.L., 1993. Internal structure and weakening mechanisms of the San Andreas Fault. Journal of Geophysical Research 98, 771–786.

Cornelius, H.P., 1935. Geologie der Err–Julier-Gruppe: Das Baumaterial. Beiträge zur geologischen Karte der Schweiz 70 (1), 1–321.

Cornelius, H.P., 1950. Geologie der Err–Julier-Gruppe: Der Gebirgsbau. Beiträge zur geologischen Karte der Schweiz 70 (2), 1–264.

Engelder, J.T., 1974. Cataclasis and the generation of fault gouge. Geological Society of American Bulletin 85, 1515–1522.

Evans, B., Dresen, G., 1991. Deformation of Earth Materials: Six Easy Pieces. Reviews of Geophysics, Supplement. U.S. National Report to International Union of Geodesy and Geophysics 1987–1990, pp. 823–843.

Evans, J.P., 1988. Deformation mechanisms in granitic rocks at shallow crustal levels. Journal of Structural Geology 10, 437–443.

Evans, J.P., 1990. Textures, deformation mechanisms, and the role of fluids in the cataclastic deformation of granitic rocks. In: Knipe, R.J., Rutter, E.H. (Eds.), Deformation Mechanisms, Rheology and Tectonics, 54. Geological Society Special Publication, pp. 29–39.

Evans, J.P., Chester, F.M., 1995. Fluid–rock interaction in faults of the San Andreas system: Inferences from San Gabriel fault rock geochemistry and microstructures. Journal of Geophysical Research 100, 13007–13020.

Evans, J.P., Forster, C.B., Goddard, J.V., 1997. Permeability of fault-related rocks, and implications for hydraulic structure of fault zones. Journal of Structural Geology 19, 1393–1404.

Fitz Gerald, J.D., Stünitz, H., 1993. Deformation of granitoids at

low metamorphic grade. I: Reactions and grain size reduction. Tectonophysics 221, 269–297.

Froitzheim, N., Eberli, G.P., 1990. Extensional detachment faulting in the evolution of a Tethys passive continental margin, Eastern Alps, Switzerland. Geological Society of America Bulletin 102, 1297–1308.

Froitzheim, N., Manatschal, G., 1996. Kinematic model for Jurassic rifting, mantle exhumation, and passive-margin formation in the Austroalpine and Penninic nappes (Eastern Switzerland). Geological Society of America Bulletin 108, 1120–1133.

Froitzheim, N., Schmid, S.M., Conti, P., 1994. Repeated change from crustal shortening to orogen-parallel extension in the Austroalpine units of Graubünden. Eclogae Geologicae Helvetiae 87, 559–612.

Groshong, R.H., 1988. Low-temperature deformation mechanisms and their interpretation. Geological Society of America Bulletin 100, 1329–1360.

Handy, M.R., 1990. The solid-state flow of polymineralic rocks. Journal of Geophysical Research 95, 8647–8661.

Handy, M.R., Herwegh, M., Regli, R., 1993. Tektonische Entwicklung der westlichen Zone von Samedan (Oberhalbstein, Graubünden, Schweiz). Eclogae Geologicae Helvetiae 86, 785–818.

Heitzmann, P., 1985. Kakirite, Kataklasite, Mylonite—Zur Nomenklatur der Metamorphite mit Verformungsgefüge. Eclogae Geologicae Helvetiae 78, 273–286.

Jordan, P., 1987. The deformational behaviour of bimineralic limestone–halite aggregates. Tectonophysics 135, 185–197.

Maddock, R.M., 1986. Frictional melting in landslide-generated frictionites (hyalomylonites) and fault-generated pseudotachylites. Discussion. Tectonophysics 128, 151–153.

Maddock, R.H., Grocott, J., van Nes, M., 1987. Vesicles, amygdales and similar structures in fault-generated pseudotachylites. Lithos 20, 419–432.

Magloughlin, J.F., Spray, J.G., 1992. Frictional melting processes and products in geological materials. Tectonophysics 204, 197–337.

Manatschal, G., 1995. Jurassic rifting and formation of a passive continental margin (Platta and Err nappes, Eastern Switzerland): geometry, kinematics and geochemistry of fault rocks and a comparison with the Galicia margin. PhD thesis, Eidgenössische Technische Hochschule, Zürich.

Manatschal, G., Nievergelt, P., 1997. A continent–ocean transition recorded in the Err and Platta nappes (Austroalpine and Penninic nappes, Eastern Switzerland). Eclogae Geologicae Helvetiae 90, 3–27.

Manatschal, G., Marquer, D., Früh-Green, G.L., in press. Channelized fluid flow and mass transfer along a rift-related detachment fault (Eastern Alps, SE Switzerland). Geological Society of America Bulletin.

Miller, S.A., Nur, A., Olgaard, D.L., 1996. Earthquakes as a coupled shear stress–high pore pressure dynamical system. Geophysical Research Letters 23, 197–200.

Neuzil, C.E., 1994. How permeable are clays and shales? Water Resource Research 30, 145–150.

Passchier, C.W., Trouw, R.A.J., 1996. Microtectonics. Springer-Verlag, Berlin.

Philpotts, A.R., 1964. Origin of pseudotachylites. American Journal of Sciences 262, 1008–1035.

Reynolds, S.J., Lister, G.S., 1987. Structural aspects of fluid–rock interactions in detachment zones. Geology 15, 362–366.

Rutter, E.H., 1986. On the nomenclature of mode of failure transitions in rocks. Tectonophysics 122, 381–387.

Rutter, E.H., Maddock, R.H., Hall, S.H., White, S.H., 1986. Comparative microstructures of natural and experimentally produced clay-bearing fault gouges. Pure and Applied Geophysics 124, 3–30.

Sammis, C.G., Osborne, R.H., Anderson, J.L., Banerdt, M., White, P., 1986. Self-similar cataclasis in the formation of fault gouge. Pure and Applied Geophysics 124, 53–78.

Schmid, S.M., Handy, M.R., 1991. Towards a genetic classification of fault rocks: geological usage and tectonophysical implications. In: Müller, D.W., McKenzie, J.A., Weissert, H. (Eds.), Controversies in Modern Geology. Academic Press, London, pp. 339–361.

Scholz, C.H., 1987. Wear and gouge formation in brittle faulting. Geology 15, 493–495.

Shimamoto, T., Nagahama, H., 1992. An argument against the crush origin of pseudotachylites based on the analysis of clast-size distribution. Journal of Structural Geology 14, 999–1006.

Sibson, R.H., 1975. Generation of pseudotachylite by ancient seismic faulting. Geophysical Journal of the Royal Astronomic Society 43, 775–794.

Stöcklin, J., 1949. Zur Geologie der nördlichen Errgruppe zwischen Val d'Err und Weissenstein (Graubünden). PhD thesis, Eidgenössische Technische Hochschule, Zürich, Universitätsverlag Wagner, Innsbruck.

Toyoshima, T., 1990. Pseudotachylite from the main zone of the Hidaka metamorphic belt, Hokkaido, northern Japan. Journal of Metamorphic Geology 9, 507–523.

Wernicke, B., 1995. Low-angle normal faults and seismicity: A review. Journal of Geophysical Research 100, 20159–20174.

Wintsch, R.P., Christoffersen, R., Kronenberg, A.K., 1995. Fluid–rock reaction weakening of fault zones. Journal of Geophysical Research 100, 13021–13032.